The Plant Cell, Vol. 8, 137–153, February 1996

RESEARCH ARTICLE

The *AINTEGUMENTA* Gene of Arabidopsis Required for Ovule and Female Gametophyte Development Is Related to the Floral Homeotic Gene *APETALA2*

Kevin M. Klucher, Helen Chow, Leonore Reiser, and Robert L. Fischer[1]

Department of Plant Biology, 111 Koshland Hall, University of California–Berkeley, Berkeley, California 94720

Ovules play a central role in plant reproduction, generating the female gametophyte within sporophytic integuments. When fertilized, the integuments differentiate into the seed coat and support the development of the embryo and endosperm. Mutations in the *AINTEGUMENTA* (*ANT*) locus of Arabidopsis have a profound effect on ovule development. Strong *ant* mutants have ovules that fail to form integuments or a female gametophyte. Flower development is also altered, with a random reduction of organs in the outer three whorls. In addition, organs present in the outer three floral whorls often have abnormal morphology. Ovules from a weak *ant* mutant contain both inner and outer integuments but generally fail to produce a functional female gametophyte. We isolated the *ANT* gene by using a mutation derived by T-DNA insertional mutagenesis. *ANT* is a member of a gene family that includes the floral homeotic gene *APETALA2* (*AP2*). Like AP2, ANT contains two AP2 domains homologous with the DNA binding domain of ethylene response element binding proteins. *ANT* is expressed most highly in developing flowers but is also expressed in vegetative tissue. Taken together, these results suggest that ANT is a transcription factor that plays a critical role in regulating ovule and female gametophyte development.

INTRODUCTION

A unique element of plant reproduction is the alternation of generations between a diploid sporophyte and a haploid gametophyte. Ovules are fundamentally involved in this aspect of the plant life cycle due to their role in generating the female gametophyte or embryo sac. Ovule development has been proposed to occur in four distinct phases (Schneitz et al., 1995). The first phase involves the initiation of the ovule primordia from the carpel placenta. During the second phase, the specification of ovule identity occurs. This is followed by the formation of spatially defined pattern elements within the developing ovule in the third phase. The final phase involves morphogenesis to form the mature ovule. In angiosperms, morphogenesis results in ovules that consist of a nucellus enclosed by one or two integuments and a supporting stalk, the funiculus, which attaches the ovule to the placenta (Bouman, 1984; Reiser and Fischer, 1993). The megasporocyte is produced within the nucellus and undergoes meiosis to produce four megaspores (megasporogenesis). A single surviving megaspore will undergo megagametogenesis to produce the female gametophyte (Willemse and Van Went, 1984; Mansfield et al., 1990; Reiser and Fischer, 1993).

Little is known about the molecular basis of ovule development. Recently, several laboratories have taken a genetic approach to understand the genetic circuitry used in the developing ovule and to identify potential communication between the diploid ovule and the haploid female gametophyte. A number of sporophytic mutants have been identified in Arabidopsis that specifically affect the ovule and/or the female gametophyte. In *bell1* (*bel1*) plants, ovules lack an inner integument, the outer integument develops abnormally, and the embryo sac arrests at a late stage in megagametogenesis (Robinson-Beers et al., 1992; Modrusan et al., 1994; Ray et al., 1994). The abnormal outer integument occasionally undergoes a homeotic transformation to a carpel-like structure late in *bel1* ovule development (Modrusan et al., 1994; Ray et al., 1994). Integument development is also altered in *short integuments1* (*sin1*) ovules. Both the inner and outer integuments are affected in *sin1* plants, and the development of the female gametophyte is arrested before megagametogenesis (Robinson-Beers et al., 1992; Lang et al., 1994). The *aberrant testa shape* (*ats*) mutant also has abnormal integument development, with no clear distinction between the developing inner and outer integuments (Léon-Kloosterziel et al., 1994). However, in contrast to *bel1* and *sin1*, the female gametophyte in the *ats* mutant is not greatly affected, with only a slight reduction in the number of mature seed generated. Two recently described ovule mutants, 47H4 and 54D12, have apparently normal ovule morphology, but viable embryo sacs are not formed (Hulskamp et al., 1995).

[1] To whom correspondence should be addressed.

Arabidopsis mutants that affect both flower and ovule development have also been identified. *APETALA2* (*AP2*) is involved in the regulation of floral meristem and organ identity (Komaki et al., 1988; Bowman et al., 1989, 1991, 1993; Kunst et al., 1989; Irish and Sussex, 1990; Shannon and Meeks-Wagner, 1993). Strong *ap2* mutants have a homeotic transformation of the first whorl organs into ovule-bearing carpels, a reduction in the number of second and third whorl organs, and defective carpel fusion in the fourth whorl (Komaki et al., 1988; Kunst et al., 1989; Bowman et al., 1991; Jofuku et al., 1994). In addition, strong *ap2* mutants have altered ovule development, producing carpel-like structures in the place of some ovules (Modrusan et al., 1994). Seed coat development is also abnormal in *ap2* mutants (Jofuku et al., 1994; Léon-Kloosterziel et al., 1994). In *superman* (*sup*) mutants, flowers with supernumerary stamens and reduced carpels are formed as a result of ectopic expression of the *APETALA3* gene (Bowman et al., 1992). Recently, *SUP* was also found to play a role in the regulation of ovule development. Mutations in the *sup* locus alter the normally asymmetric growth of the outer integument to form a tubelike structure with nearly radial symmetry (Gaiser et al., 1995).

How do the genes described above work to form a functional ovule and female gametophyte? In some cases, these genes act as transcriptional regulators. Recently, Reiser et al. (1995) isolated the *BEL1* gene and found that it encodes a homeodomain protein localized in the nucleus. Early *BEL1* gene expression in the ovule was found to be restricted to the region in which the integuments will form, suggesting that the spatial accumulation of *BEL1* RNA marks a domain for integument primordium initiation (Reiser et al., 1995). The *AP2* gene encodes a putative nuclear protein containing two copies of a novel 68–amino acid motif designated the AP2 domain (Jofuku et al., 1994). The AP2 domain is related to the DNA binding region of ethylene response element binding proteins, a family of proteins involved in ethylene signal transduction (Ecker, 1995; Ohme-Takagi and Shinshi, 1995; Weigel, 1995). The *AP2* gene is expressed throughout flower development in all four types of floral organs and the developing ovule (Jofuku et al., 1994).

In this report, we describe the development of ovules from *aintegumenta* (*ant*), an Arabidopsis mutant defective in integument and female gametophyte development. We cloned the *ANT* gene and show that it is related to a family of genes encoding AP2 domain proteins. Finally, we show that, similar to *AP2*, *ANT* gene expression is not restricted to floral tissue but is also expressed in vegetative organs.

RESULTS

Isolation of *ant* Alleles

Approximately 8000 Arabidopsis lines transformed with the T-DNA of Agrobacterium (Feldmann, 1991) were screened for mutations that reduce fertility on the basis of reduced silique size. Two lines showing reduced fertility were determined to be female sterile by reciprocal crosses to wild-type plants. Analysis of F_2 segregating populations indicated that the sterile phenotype was due to a single recessive nuclear mutation, and complementation tests indicated that the two lines were allelic (see Methods). A third allele was isolated independently in another screen of these lines (G. Haughn, personal communication). We named this mutant *ant* due to the ovule phenotype described below. The three alleles were designated *ant-1*, *ant-2*, and *ant-3*.

The map position of the *ANT* gene was determined by genetic crosses to marker lines. Analysis of 400 F_2 progeny of the cross *ant-3* with the chromosome 4 markers *brevipedicellus* (*bp*), *eceriferium2* (*cer2*), and *ap2* indicated that *ANT* is genetically linked to *AP2* on chromosome 4 (see Methods).

Ovule Development in *ant* Plants Is Abnormal

To determine the cause of the sterile phenotype in *ant* mutants, we analyzed the morphology and anatomy of ovules from *ant* plants. Figures 1 and 2 show the results of scanning electron microscopy and light microscopy, respectively, of critical stages in the development of *ant-1* and *ant-3* ovules.

ant-1 Ovule Development

Detailed analyses of Arabidopsis ovule development have been reported previously (Robinson-Beers et al., 1992; Modrusan et al., 1994; Schneitz et al., 1995). Wild-type ovule primordia initiate from the placental tissue located at the carpel margins during stage 8 of wild-type flower development (flower staging based on Smyth et al., 1990). These primordia continue to enlarge during stage 9, as shown in Figure 1A. The inner and then the outer integuments both initiate by periclinal divisions of epidermal cells during stage 10 of flower development. These divisions spread circumferentially around the ovule, forming a ring that delimits the nucellus as the apical portion of the primordium (Figure 1D). Integument growth continues during stages 11 and 12 (Figure 1G), fully enclosing the nucellus by late stage 12. The outer integument undergoes asymmetric growth, eventually overgrowing the inner integument and forming the micropylar opening (Figure 1J). The megasporocyte can be distinguished within the nucellus by stage 9 in wild-type ovules (Figure 2A). Megasporogenesis begins during stage 10, the same time as integument initiation. This produces a linear tetrad of megaspores of which only the chalazal megaspore survives (Figure 2D). During stage 12, the surviving megaspore undergoes megagametogenesis to form the seven-celled, eight-nucleate female gametophyte present at maturity (Figure 2G).

No defects in *ant-1* ovules were detected during the earliest stages of development. Similar to the wild type, ovule primordia in the *ant-1* mutant initiate during stage 8 (data not shown) and enlarge during stage 9 (Figure 1B). However, initiation of integument growth does not occur during stage 10 (Figure 1E)

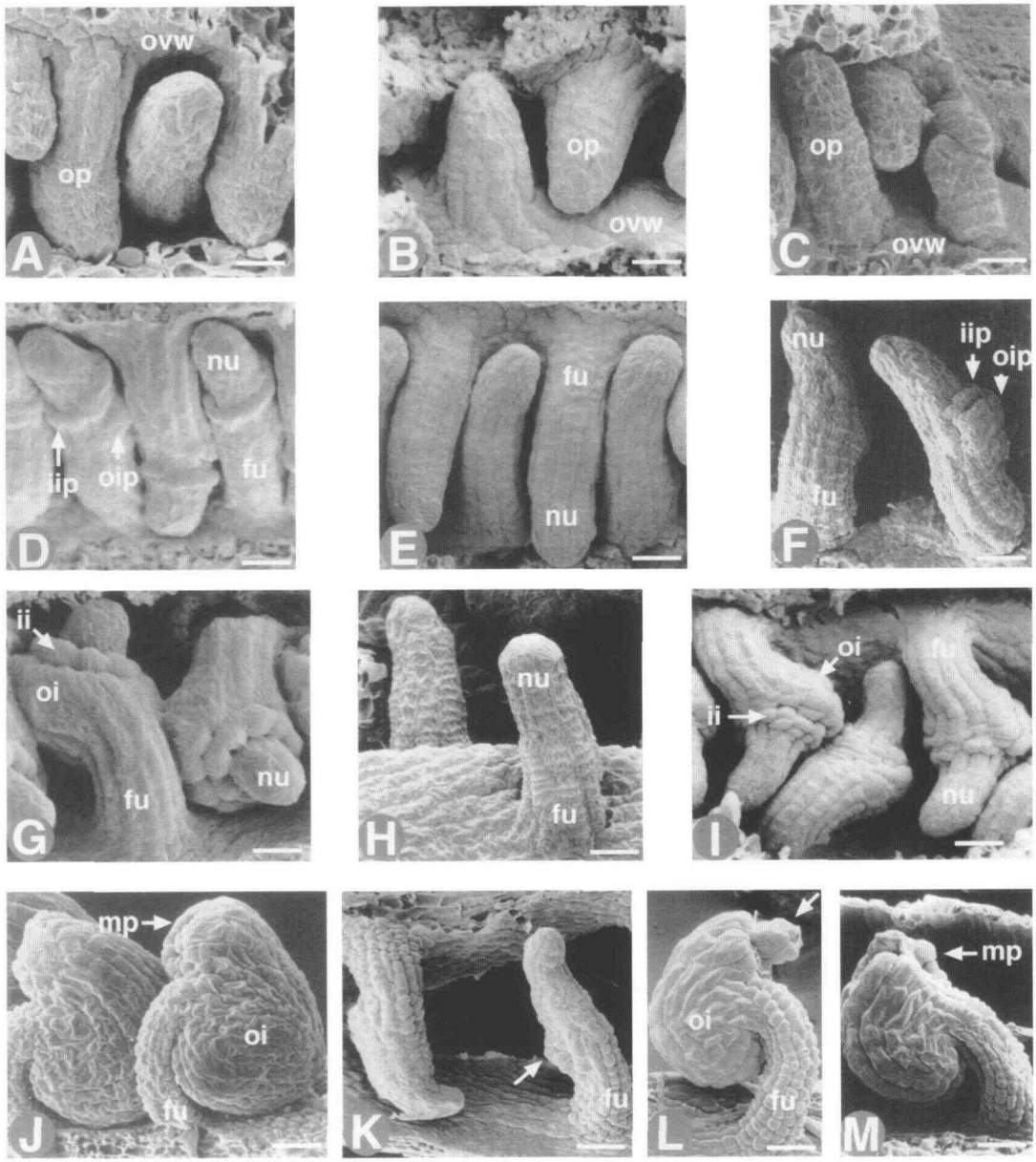

Figure 1. Scanning Electron Microscopy of Developing Wild-Type, *ant-1*, and *ant-3* Ovules.

(A) Developing ovule primordia from a stage 9 wild-type carpel. Bar = 10 μm.
(B) Developing ovule primordia from a stage 9 *ant-1* carpel. Bar = 10 μm.
(C) Developing ovule primordia from a stage 9 *ant-3* carpel. Bar = 10 μm.
(D) Elongated ovule primordia from a stage 10 wild-type carpel. Ovule primordia differentiate into a nucellus and funiculus delimited by the initiation of the inner and outer integument primordia. Bar = 13 μm.
(E) Elongated ovule primordia from a stage 10 *ant-1* carpel. Bar = 13 μm.
(F) Elongated ovule primordia from a stage 10 *ant-3* carpel. The initiation of the inner and outer integument primordia on one side of the ovule is shown. Bar = 13 μm.
(G) Developing ovule from a stage 11 wild-type carpel showing the expanding inner and outer integuments. Bar = 13 μm.
(H) Developing ovule from a stage 11 *ant-1* carpel is shown. Bar = 13 μm.
(I) Developing ovule from a stage 11 *ant-3* carpel. The expanding inner and outer integuments are shown. Bar = 13 μm.
(J) Mature ovules from a stage 13 wild-type carpel are shown. The arrow indicates the micropylar opening. Bar = 24 μm.
(K) Ovules from a stage 13 *ant-1* carpel. The arrow indicates the ridge of cells possibly representing integument growth. Bar = 23 μm.
(L) Mature ovule from stage 13 *ant-3* carpel. The arrow indicates the protuberance from the micropylar opening. Bar = 23 μm.
(M) Mature ovule from a stage 13 *ant-3* carpel is shown. The arrow indicates the micropylar opening. Bar = 23 μm.
fu, funiculus; ii, integument; iip, integument primordia; mp, micropylar opening; nu, nucellus; oi, outer integument; oip, outer integument primordia; op, ovule primordia; ovw, ovary wall.

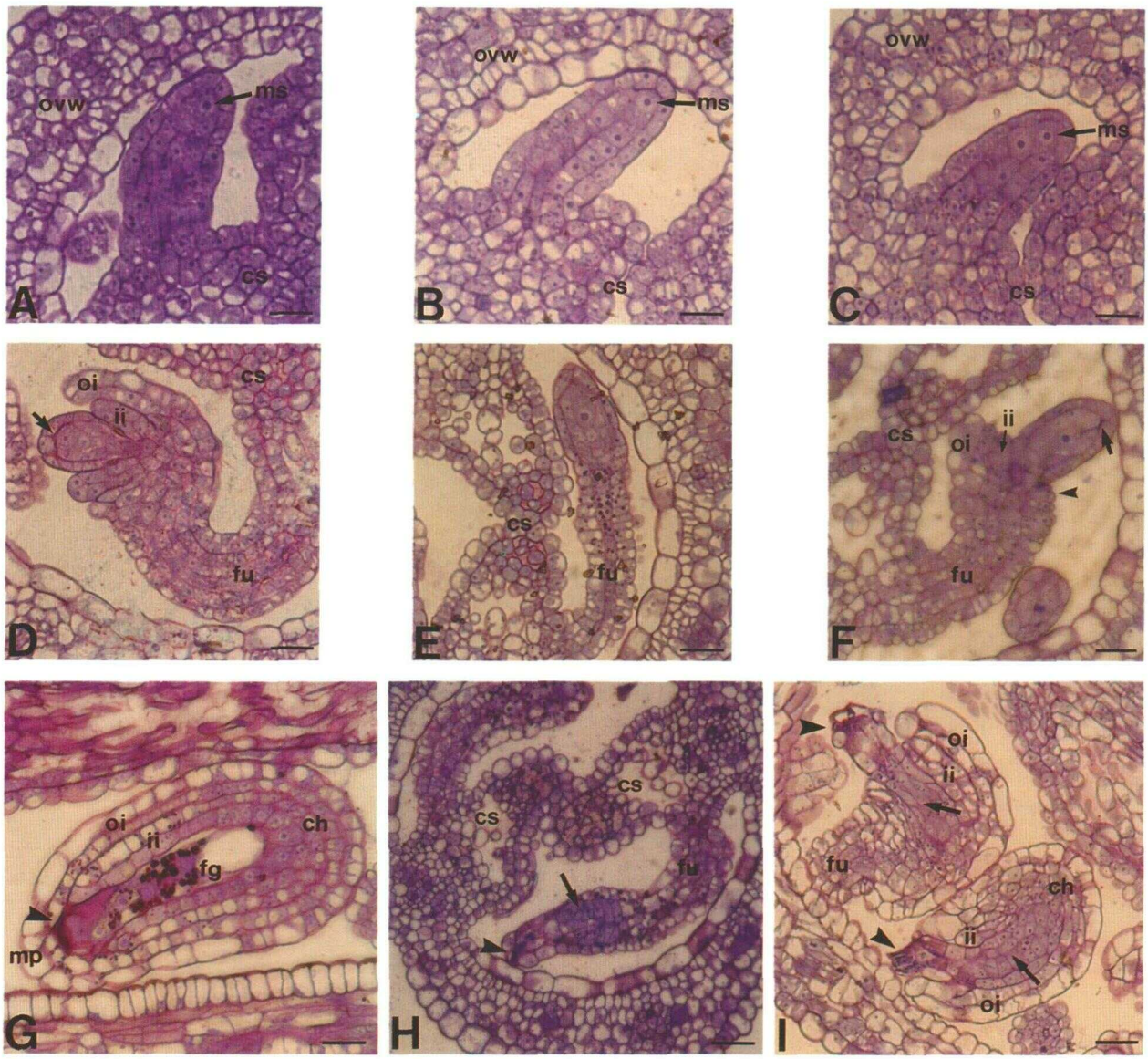

Figure 2. Light Microscopy of Developing Wild-Type, *ant-1*, and *ant-3* Ovules.

(A) Developing ovule primordia from a stage 9 wild-type carpel. The megasporocyte is indicated by the arrow. Bar = 7 μm.
(B) Developing ovule primordia from a stage 9 *ant-1* carpel. The megasporocyte is indicated by the arrow. Bar = 7 μm.
(C) Developing ovule primordia from a stage 9 *ant-3* carpel. The megasporocyte is indicated by the arrow. Bar = 7 μm.
(D) Developing ovule from a stage 11 wild-type carpel showing the expanding inner and outer integuments. The arrow indicates the densely staining cells of the linear tetrad that are degenerating. Bar = 9 μm.
(E) Developing ovule from a stage 11 *ant-1* carpel. Bar = 9 μm.
(F) Developing ovule from a stage 11 *ant-3* carpel showing the expanding inner and outer integuments. The arrowhead indicates the underdeveloped integuments on one side of the ovule. Densely staining cells of the linear tetrad that are degenerating are shown by the arrow. Bar = 9 μm.
(G) Mature ovule from a stage 13 wild-type carpel showing the fully developed inner and outer integuments. The female gametophyte is found in the center of the ovule. The arrowhead indicates the densely staining tissue near the micropyle. Bar = 12 μm.
(H) Ovules from a stage 13 *ant-1* carpel with the abnormal proliferation of cells in the nucellus, which is shown by the arrow. The arrowhead indicates the densely staining tissue near the micropyle. Bar = 12 μm.
(I) Mature ovules from a stage 13 *ant-3* carpel. The arrows indicate the abnormal proliferation of cells in the ovule nucellus. The densely staining tissue near the micropyles is shown by the arrowheads. Bar = 12 μm.
ch, chalaza; cs, central septum; fg, female gametophyte; fu, funiculus; ii, inner integument; mp, micropyle; ms, megasporocyte; oi, outer integument; ovw, ovary wall.

or at later times during development (Figure 1H). Occasionally, mature *ant-1* ovules contain a ridge of tissue in the approximate position of wild-type integument initiation (Figure 1K), but this tissue does not develop further. A periclinal division of an epidermal cell is also sometimes seen in *ant-1* ovules and is similar to that seen during wild-type integument initiation; however, continued cell division does not occur (data not shown).

As in wild-type ovules, a megasporocyte is detected within the nucellus of *ant-1* ovules by stage 9 (Figure 2B). However, further development of a female gametophyte does not appear to occur (Figures 2E and 2H). Instead, a proliferation of similarly staining cells is found in the nucellus adjacent to the funiculus (Figure 2H). A densely staining region is located at the tip of the ovule (Figure 2H). A similar region is seen in wild-type ovules at the micropylar end (Figure 2G).

In addition to the defective ovule development, aberrant development of the central septum is often seen in the *ant-1* carpel. In wild-type pistil development, septal tissue grows symmetrically from opposite sides of the developing gynoecium, meeting in the center, where they fuse postgenitally (data not shown; Hill and Lord, 1989). In contrast, growth of *ant-1* septal tissue is often asymmetric, resulting in abnormal fusion of the central septal tissue (Figure 2H).

ant-3 Ovule Development

As found in wild-type ovule development, *ant-3* ovule primordia initiate during stage 8 (data not shown) and enlarge during stage 9 (Figure 1C). Although integument initiation occurs during stage 10 in *ant-3* ovules, the initiation is abnormal. In contrast to the rings of integuments around the wild-type ovule at this stage (Figure 1D), initiation and some growth of both the inner and outer integuments occur primarily on one side of the *ant-3* ovule (Figures 1F and 2F). As development proceeds, both the inner and outer integuments surround the nucellus (Figures 1I and 2I), although the boundary between the inner and outer integuments is less clear than in the wild type. The growth of *ant-3* integuments is variable, but in general, the integuments are both shorter and smaller than in wild-type ovules (compare Figure 1J with Figures 1L and 1M, and Figure 2G with Figure 2I). In some *ant-3* ovules, the nucellus protrudes from the micropylar end (Figures 1L and 2I).

A megasporocyte can be seen in the *ant-3* nucellus by stage 9 (Figure 2C), as in wild-type ovules. Megasporogenesis appears to occur, and a single megaspore enlarges (Figure 2F). However, in contrast to the wild type, the surviving megaspore does not normally undergo megagametogenesis. Instead, the nucellus displays an abnormal proliferation of cells in the region normally occupied by the female gametophyte (Figure 2I), similar to that described in *ant-1* ovules (Figure 2H). A densely staining region is located at the micropylar end of the ovule (Figure 2I), as seen in both wild-type and *ant-1* ovules. Although the great majority of *ant-3* ovules failed to develop a female gametophyte, a small percentage of ovules (<0.2% of wild type) generated viable seed (Table 1).

Based on the severity of the ovule phenotype, we have designated *ant-1* as a strong mutant and *ant-3* as a weak mutant. Preliminary analysis indicates that *ant-2* can also be classified as a strong mutant (K. Klucher, unpublished results). As discussed below, the phenotypic assignment of mutant strength was confirmed by molecular analysis.

Interaction between *ANT* and *BEL1*

To begin to understand the relationship of *ANT* to other genes involved in ovule development, we analyzed the interaction between *ANT* and *BEL1*. *BEL1* affects the development of both the inner and outer integuments, although in different ways. Ovules from *bel1* mutants lack an inner integument. The outer integument appears to initiate but develops abnormally and never resembles a wild-type outer integument at any time during development (Robinson-Beers et al., 1992; Modrusan et al., 1994; Ray et al., 1994). This suggests that *BEL1* has at least two roles: it is a regulator of inner integument initiation and specifies proper organ identity in the outer integument. In contrast, *ANT* appears to be required for integument initiation in general and does not appear to play a role in organ identity in the ovule. This suggests that *ANT* should be necessary not only for wild-type integument initiation but also for the initiation of the abnormal integument-like structure found in *bel1* ovules. To test this hypothesis, *ant-1 bel1-2* double mutants were constructed and analyzed for integument development. As shown in Figure 3A, *bel1-2* ovules contain the characteristic bell-like collar of tissue that forms the single integument-like structure. In contrast, ovules from the *ant-1 bel1-2* double mutant (Figure 3B) resemble *ant-1* ovules, failing to form either inner or outer integument (Figure 1K). This result indicates that *ANT* is required for the initiation of the abnormal integument-like structure found in *bel1* ovules as well as for inner and outer integument initiation in wild-type ovules.

It has been shown recently that the spatial accumulation of *BEL1* RNA marks a domain for integument primordium initiation (Reiser et al., 1995). To determine whether the absence of integument development in strong *ant* mutants was due to altered *BEL1* gene expression, in situ hybridization of *ant-1* ovules with a *BEL1* antisense RNA probe was performed. In wild-type plants, *BEL1* RNA was detected in stage 9 ovules before integument initiation (Figure 3C). *BEL1* RNA accumulation

Table 1. Complementation of *ant-3* Plants

Line	Seed/Silique[a]
Wild type	46.4 ± 3.9 (n = 5)
2B	5.1 ± 2.4 (n = 23)
3C	5.5 ± 1.8 (n = 20)
5E	5.5 ± 2.7 (n = 20)
ant-3	0.1 ± 0.3 (n = 80)

[a] The average ± SD for the indicated number of siliques (n) is given.

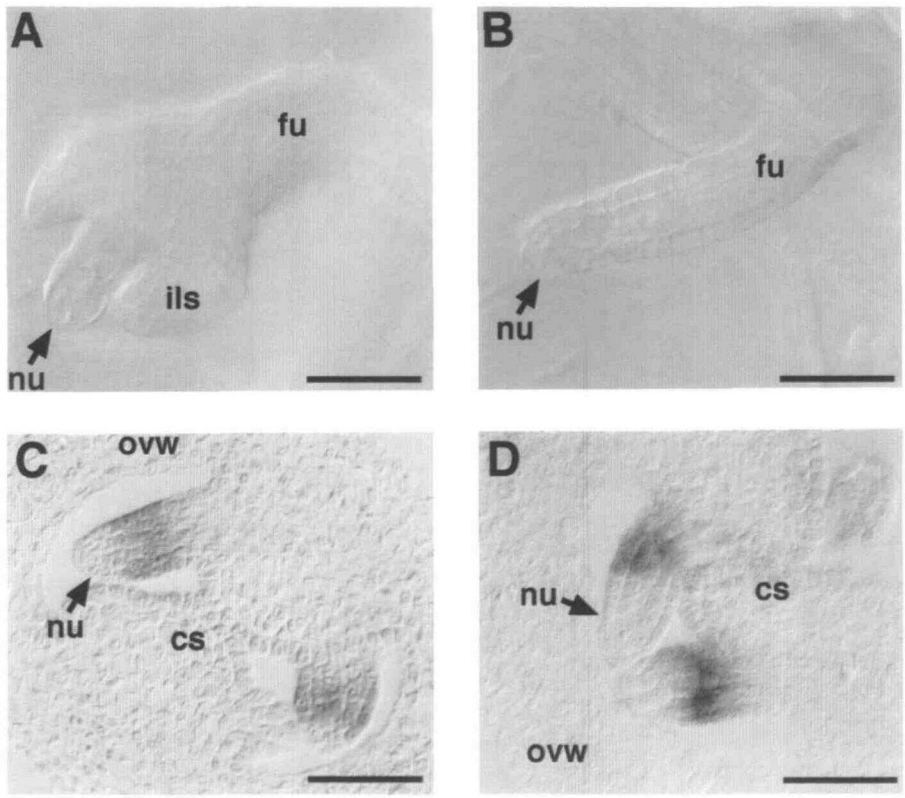

Figure 3. Analysis of Interactions between *ANT* and *BEL1*.

(A) Cleared stage 13 ovule from a *bel1-2* plant viewed with differential interference contrast optics. Bar = 42 μm.
(B) Cleared stage 13 ovule from an *ant-1 bel1-2* double mutant plant viewed with differential interference contrast optics. Bar = 42 μm.
(C) In situ hybridization of stage 9 wild-type ovules, using a *BEL1* antisense RNA probe. Bar = 37 μm.
(D) In situ hybridization of stage 9 *ant-1* ovules, using a *BEL1* antisense RNA probe. Bar = 37 μm.
cs, central septum; fu, funiculus; ils, integument-like structure; nu, nucellus; ovw, ovary wall.

appears to be restricted to the region in which the integument primordia will initiate during stage 10 (compare Figure 3C with Figure 1D). A similar pattern of *BEL1* RNA accumulation is seen in *ant-1* ovules (Figure 3D), with *BEL1* RNA detected at stage 9 near the position where the integuments would develop in wild-type ovules. These results indicate that, although strong *ant* mutants fail to initiate inner and outer integuments, an integument-specific domain, as defined by the region of *BEL1* RNA accumulation, is still produced.

Development Is Altered in All Floral Whorls of Strong *ant* Mutants

In addition to the effects on ovule development, both strong *ant* mutants, *ant-1* and *ant-2*, showed abnormalities in all whorls of the flower. As shown in Figure 4A, wild-type Arabidopsis flowers contain four sepals in the outer whorl, four petals in the second whorl, six stamens in the third whorl, and a congenitally fused bicarpellate gynoecium in the fourth whorl (Smyth et al., 1990). In contrast, flowers from the strong *ant-1* mutant showed varied defects in organ number and morphology (Figures 4C to 4E; see narrow petal in Figure 4D and narrow sepal in 4E).

Results of a quantitative study of the floral structures in the *ant-1* mutant are shown in Figure 5. One hundred *ant-1* flowers and 100 control wild-type flowers were scored for the number of organs in each whorl. In general, *ant-1* flowers contained three or four sepals in the first whorl (88% of *ant-1* flowers; Figure 5A). In 4% of the flowers, however, five narrow sepals were found. In addition, two or more sepals were often fully or partially fused (see sepals in Figure 4D). The majority of *ant-1* flowers contained two petals (46%), although 8% contained the normal complement of four and 6% contained none (Figure 5B). The petals that were present were always narrower and often shorter in length (Figure 4D). Most *ant-1* flowers contained four stamens, and only one flower scored contained the full complement of six stamens (Figure 5C). As with the sepals,

multiple stamens were often fused in *ant-1* flowers (data not shown). Flowers located near the apex were no more or less abnormal than more basally located flowers, and with the exception of a rare staminoid petal (data not shown), no homeotic transformations were found. Similar quantitative results were found for *ant-2* flowers (data not shown).

Flowers of the weak *ant-3* allele showed only subtle differences from the wild type (Figure 4B). A quantitative study of 100 *ant-3* flowers indicated that only one flower contained three sepals in the first whorl, with the remaining having four (Figure 5A). Ninety-six percent of the flowers contained four morphologically normal petals (Figure 5B). The average number of stamens was slightly reduced in *ant-3* flowers compared with the wild type, with an average of approximately five stamens per flower (Figure 5C).

Molecular Cloning of *ANT*

DNA gel blot analysis of the three *ant* alleles indicated that only *ant-3* contains a T-DNA that cosegregates with the sterile phenotype (data not shown). A genomic library was constructed

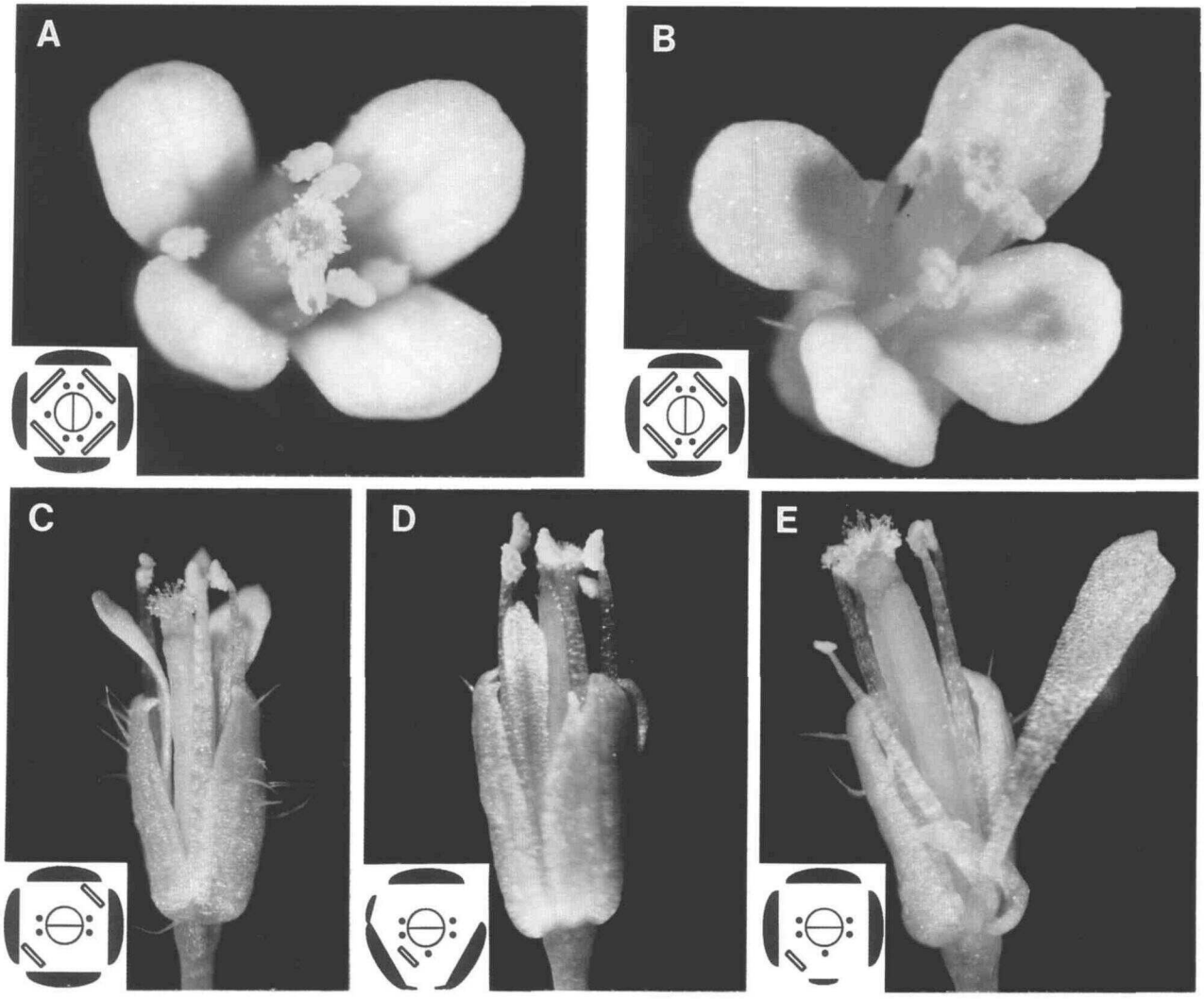

Figure 4. Flower Morphology of *ant* Mutants.

Flowers from wild-type, *ant-3*, and *ant-1* plants are shown with a schematic flower diagram.
(A) Wild-type flower.
(B) *ant-3* flower.
(C) to **(E)** *ant-1* flowers.
For the schematic flower diagram, the outer half ovals represent sepals, the lines represent petals, the black circles represent stamens, and the innermost circle represents the carpel.

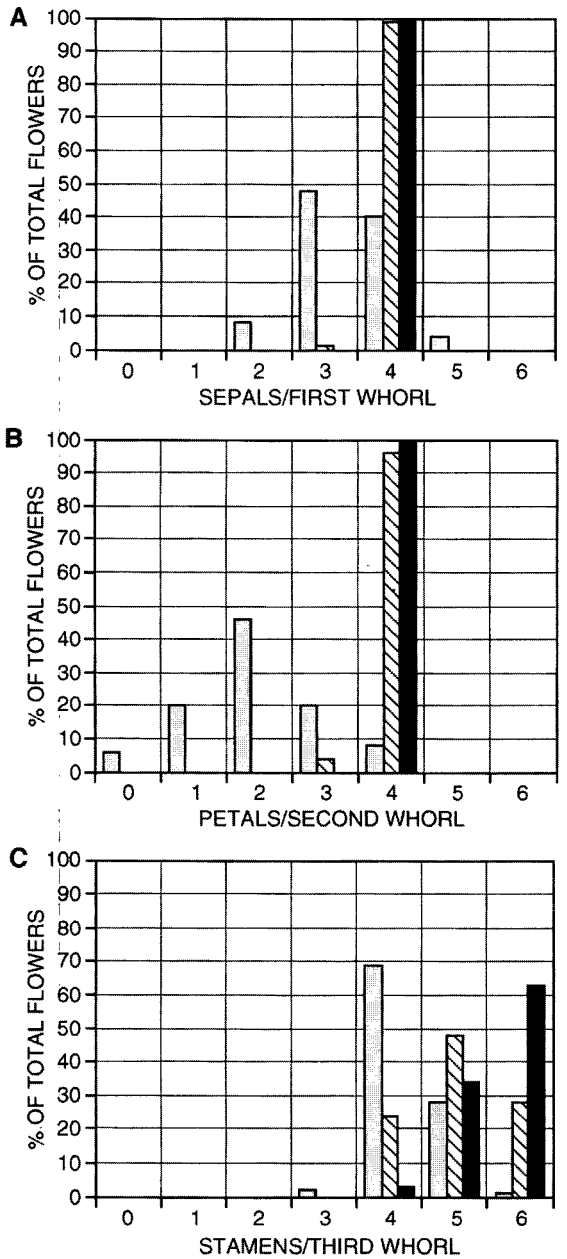

Figure 5. Quantification of *ant* Floral Organs.

A total of 100 *ant-1* flowers from eight plants, 100 *ant-3* flowers from 12 plants, and 100 wild-type flowers from five plants were scored for the number of organs in each of the outer three whorls of the flower. The percentage of total flowers with the indicated number of organs per whorl is shown. Gray bars indicate *ant-1* flowers, striped bars indicate *ant-3* flowers, and black bars indicate wild-type flowers.

(A) The percentage of total flowers from *ant-1*, *ant-3*, and wild-type plants with the indicated number of sepals per first whorl is shown.

(B) The percentage of total flowers from *ant-1*, *ant-3*, and wild-type plants with the indicated number of petals per second whorl is shown.

(C) The percentage of total flowers from *ant-1*, *ant-3*, and wild-type plants with the indicated number of stamens per third whorl is shown.

with DNA from homozygous *ant-3* plants and screened with probes containing the right and left T-DNA borders. Plant sequences flanking the T-DNA tag were obtained and used to screen a wild-type genomic library. A map of the wild-type genomic region is shown in Figure 6. The location of the T-DNA insertion in the *ant-3* allele is indicated on the map.

To confirm that we had identified the *ANT* genomic region, we transformed homozygous *ant-3* plants with a 10-kb wild-type genomic fragment spanning the site of the T-DNA insertion in *ant-3* (pKK18 in Figure 6). Three independent transformed lines were obtained (lines 2B, 3C, and 5E), and fertile progeny of the primary transformants from each line were scored for seed set. Table 1 shows that all three transformed lines were ~50 to 60 times more fertile than the *ant-3* mutant and approximately eight- to ninefold less fertile than the wild-type plants. Progeny of the primary transformants segregated fertile and sterile plants in a 3:1 ratio (36 fertile:12 sterile for line 2B), suggesting single insertional events, and the transgene segregated with fertility (data not shown). In addition to seed development, some development of the silique was also found (data not shown). Taken together, these results indicate that the 10-kb transgenic region introduced was responsible for the partial restoration of fertility and likely contains the *ANT* gene. As discussed below, sequence analysis of *ant-1* and *ant-2* confirmed this conclusion.

Characterization of the *ANT* Gene

Plant sequences immediately flanking the T-DNA in *ant-3* did not detect any transcribed sequences within RNA from developing wild-type flowers (data not shown), suggesting that the T-DNA insertion in *ant-3* might not be within an exon of the *ANT* gene. Therefore, to identify *ANT* cDNAs, two HindIII fragments (Figure 6) fully contained within the complementing 10-kb genomic region were used to screen a flower cDNA library. Six partial clones were obtained from the ~200,000

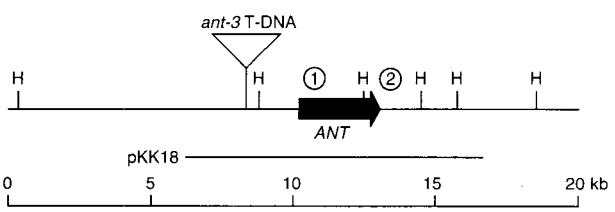

Figure 6. *ANT* Genomic Region.

A HindIII restriction map of the wild-type *ANT* genomic region is shown. The *ANT* transcription unit is indicated by the black arrow, with the arrowhead signifying the direction of transcription. The location of the T-DNA insertion in *ant-3* is shown. The HindIII fragments used for *ANT* cDNA isolation are labeled 1 and 2 on the map. The region of the genome used for complementation of the *ant-3* mutant is indicated by pKK18. H represents HindIII restriction sites.

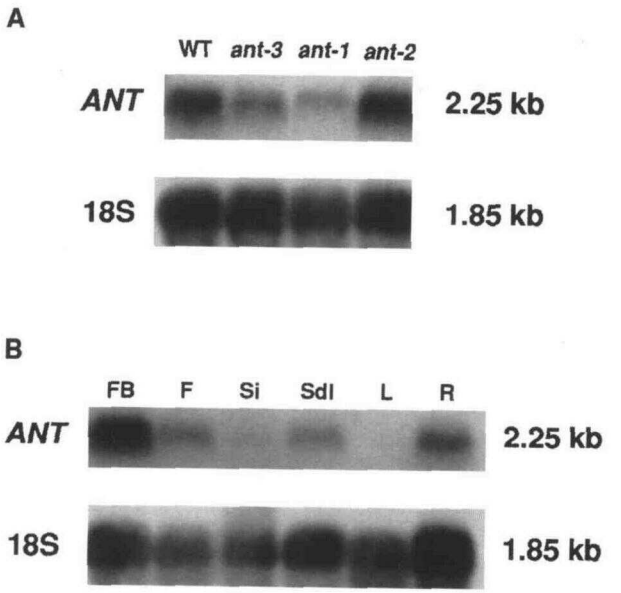

Figure 7. *ANT* Gene Expression in Mutant and Wild-Type Tissue.

(A) The accumulation of *ANT* RNA in wild-type (WT), *ant-3* , *ant-1*, and *ant-2* flower bud tissue, including the inflorescence meristem (stages 0 to 12), is shown (top). The 18S rRNA was used as a control (bottom). The sizes of the indicated transcripts are shown at the right in kilobases.
(B) The accumulation of *ANT* RNA in wild-type flower bud tissue, including the inflorescence meristem (stages 0 to 12) (FB), open flowers (stage 13) (F), young siliques (Si), aerial portion of 9-day-old seedlings (Sdl), mature rosette leaf (L), and roots from 10-day-old seedlings (R) is shown (top). The 18S rRNA was used as a control (bottom). The sizes of the indicated transcripts are shown at right in kilobases.

phage screened. As shown in Figure 7A, the longest cDNA (1.8 kb) hybridized with a 2.25-kb transcript in total RNA from developing flowers of wild-type, *ant-1*, *ant-2*, and *ant-3* plants. The transcript detected in developing flowers from the *ant-1* and *ant-3* mutants was reduced approximately two- to three-fold compared with developing flowers from wild-type and *ant-2* plants.

Rapid amplification of cDNA ends (RACE) was used to identify and clone the 5′ end of the *ANT* transcript (Frohman et al., 1988). As shown in Figure 8A, the resulting full-length cDNA is 2148 bp, in close agreement with the 2.25-kb transcript length. An open reading frame of 1665 bp beginning from the ATG at nucleotide 269 encodes a protein of 555 amino acids with a predicted molecular mass of 61.7 kD. The genomic sequence of this region was also determined, and seven introns were found within the *ANT* transcription unit (Figure 8B).

Identification of Mutations in *ant* Alleles

The molecular defects in *ant-1* and *ant-2* were identified by sequencing the *ANT* genomic DNA from these alleles. A 22-nucleotide deletion (from cDNA nucleotides 803 to 824) was found within the open reading frame of the *ant-1* allele, causing a frameshift mutation. The resulting ANT protein would be truncated by two-thirds (Figures 8A and 8B). The *ant-2* genome contained a G-to-A transition at nucleotide 1413, substituting a glycine at amino acid 382 for an aspartic acid residue (Figures 8A and 8B).

Analysis of the *ANT* genomic region indicated that the T-DNA insertion in *ant-3* was ~2 kb upstream of the *ANT* RNA start site (Figure 6). To determine whether there were other mutations within the *ANT* gene of this allele, the *ANT* genomic region in *ant-3* was sequenced. No additional mutations were found within the transcribed sequences. Therefore, the reduction in the *ANT* message (Figure 7A) is the likely cause of the greatly reduced fertility in *ant-3* plants. The identification of the molecular defects in the three *ant* alleles and the partial complementation of *ant-3* together indicate that we have isolated the *ANT* gene.

ANT Is Related to the AP2 Domain Family of Proteins

A search of the available data bases indicated that the *ANT* gene product is related to a family of proteins containing the AP2 domain. First identified in AP2, this motif is characterized by a region of ~60– to 70–amino acid residues with a highly conserved core region with the capacity to form an amphipathic α-helix (Jofuku et al., 1994; Ohme-Takagi and Shinshi, 1995). Like the *AP2* gene product, ANT contains two AP2 domains (amino acids 281 to 451) (Figures 8A and 8B), and the homology with AP2 domain proteins is restricted to this region.

As shown in Figure 9A, the AP2 domains present in ANT share between 32 and 72% amino acid identity with the AP2 domains of other family members and contain all of the previously identified invariant amino acids (Weigel, 1995). The ANT AP2 domains are most closely related to AP2 and D15799, a translated rice expressed sequence tag (EST) with no known function. D15799, like ANT and AP2, contains two AP2 domains. All members identified containing two AP2 domains also have a linker region between the domains that is conserved in both sequence and length (Figure 9B). The ANT linker shows between 52 and 60% amino acid identity with the linker regions of the other multiple AP2 domain proteins with a number of invariant amino acids. The invariant glycine residue indicated in the ANT linker by an asterisk is altered to an aspartic acid in the *ant-2* gene product.

In addition to a putative DNA binding domain, ANT contains other hallmarks of a transcription factor. A serine-threonine–rich region is found near the N terminus of ANT (amino acids 13 to 53) (Figures 8A and 8B). Sequences rich in serine and threonine have been implicated in transcriptional activation (Seipel et al., 1992; Gashler et al., 1993). A potential nuclear localization site is present within the ANT protein from amino acids 252 to 255, suggesting that ANT may be targeted to the nucleus (Figure 8A; Chelsky et al., 1989).

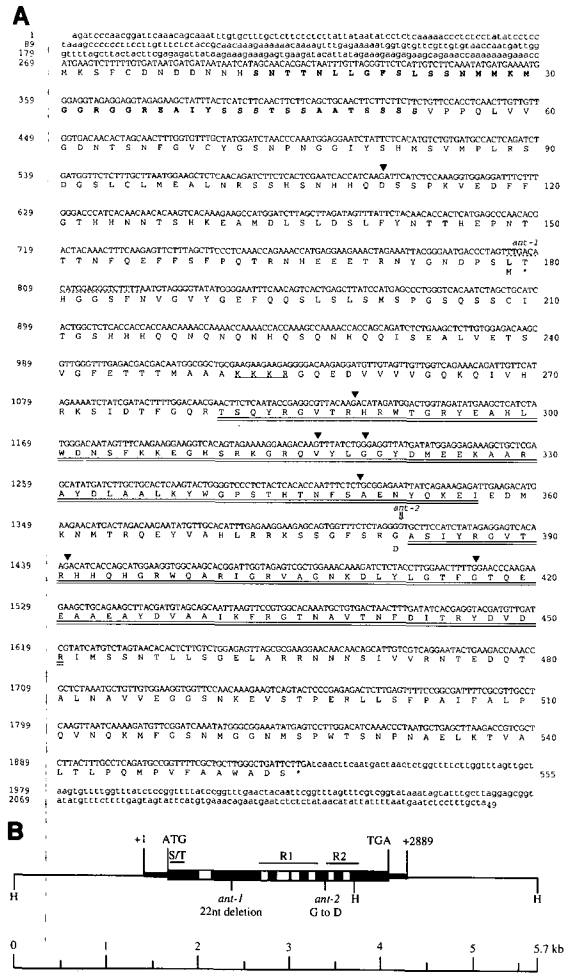

Figure 8. *ANT* cDNA Sequence and Gene Structure.

(A) The *ANT* cDNA sequence is shown. Lowercase letters indicate the 5′ and 3′ untranslated sequences. The open reading frame is indicated by uppercase letters, with the predicted amino acid sequence shown below. Asterisks indicate stop codons. The two AP2 domain repeats are double underlined. The serine-threonine–rich region is shown in boldface letters, and the putative nuclear localization site is indicated by the single underline. The locations of the *ant-1* and *ant-2* mutations are indicated above the wild-type nucleotide sequence. The 22-nucleotide deletion in *ant-1* is indicated by the dashed nucleotide sequence. The predicted alterations in the *ant-1* and *ant-2* ANT protein are shown below the wild-type amino acid sequence. The nucleotide numbering is on the left and the amino acid numbering on the right. Locations of introns within the *ANT* gene are indicated by the arrowheads above the cDNA nucleotide sequence. GenBank accession number is U40256.

(B) The *ANT* gene structure is shown. Exons and introns are represented by black and white boxes, respectively. The coding region is indicated by the thick lines. The locations of the start (ATG) and stop (TGA) codons are shown. The transcription start site (+1) was determined from the sequence of the longest 5′ RACE product and the polyadenylation site (+2889) by sequencing of the *ANT* cDNAs. The two AP2 domains are indicated by R1 and R2, and the serine-threonine–rich region by S/T. The mutations in *ant-1* and *ant-2* are shown below the gene structure. H, HindIII restriction sites; nt, nucleotide.

ANT Is Expressed in Floral and Vegetative Tissue

To identify the temporal and spatial expression patterns of the *ANT* gene, an *ANT* cDNA was hybridized at high stringency to an RNA gel blot containing total RNA from various plant organs (Figure 7B). The highest level of *ANT* expression was found in developing flowers. Expression was also detected in mature flowers and developing siliques, although at reduced levels. *ANT* RNA was also found in both the aerial and root portions of seedlings before floral induction. However, expression was not detected in mature rosette leaf (Figure 7B), young rosette, or cauline leaf tissue (data not shown).

DISCUSSION

ANT Is Required for Ovule and Female Gametophyte Development

Ovules play a pivotal role in the reproductive life cycle of plants. *ANT* is critical for the development of these organs due to its requirement for the initiation and growth of ovule integuments and the development of the female gametophyte. Ovules of strong *ant* mutants either do not initiate integument growth or have an abortive initiation after only a few cell divisions (Figures 1E, 1H, and 1K). The strong *ant-1* allele was found to contain a frameshift mutation resulting in a truncated ANT protein after only one-third of the protein has been produced. This is likely a null allele, with the effect on integument development due to the complete loss of ANT activity.

In contrast to the strong *ant* mutants, ovules of a weak mutant, *ant-3*, contain both the inner and outer integuments, although the degree of integument development is variable (Figures 1I, 1L, and 1M). The molecular defect in the *ant-3* allele is the insertion of a T-DNA in the upstream regulatory region, ~2 kb from the transcription start site. This causes a two- to three-fold reduction in the steady state levels of *ANT* RNA in developing *ant-3* flowers (Figure 7A), the putative cause of the sterile phenotype. It is not known whether the reduction in the *ANT* message seen in RNA gel blot analysis is due to an equal reduction in all floral tissue or to a much larger reduction specifically in the ovule, perhaps because of the loss of a tissue-specific promoter element. In situ localization of *ANT* gene expression in wild-type and *ant-3* flowers will address this question.

In addition to the abnormal integument development, all *ant* mutants have defective female gametophyte development

A AP2 Domain

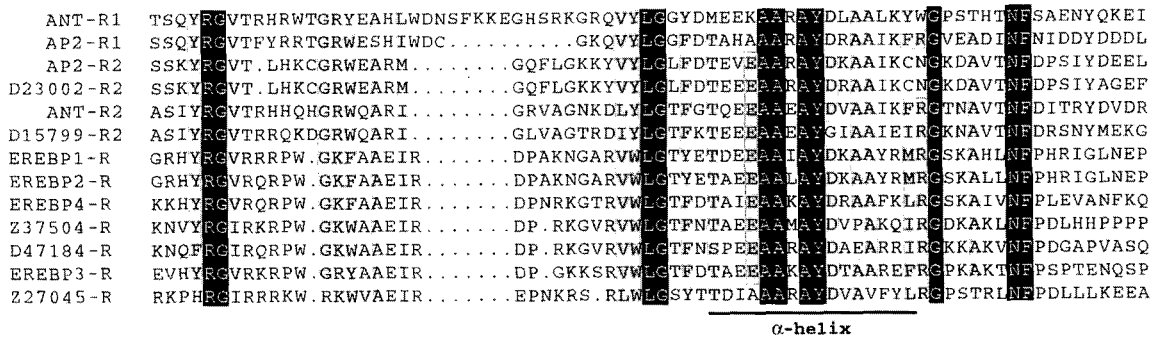

B Linker

Figure 9. ANT Is a Member of the AP2 Domain Family of Proteins.

A comparative sequence analysis of the AP2 domain **(A)** and linker region **(B)** from AP2 domain proteins is shown. Invariant amino acids in all members are indicated by black boxes. Similar amino acids are indicated by gray boxes (similarity was based on amino acids with no or conservative substitutions in at least 75% of the members). Gaps required for optimal alignment are indicated by periods. Sequence comparisons were made using the PileUp program from Genetics Computer Group (Madison, WI).

(A) AP2 domain. The highly conserved core region capable of forming an amphipathic α-helix is underlined. ANT-R1 and ANT-R2, ANT AP2 domains 1 and 2, respectively; AP2-R1 and AP2-R2, AP2 domains 1 and 2, respectively (Jofuku et al., 1994); D23002-R2 and D15799-R2, AP2 domain 2 from translated rice ESTs (GenBank accession numbers D23002 and D15799); EREBP1-R through EREBP4-R, AP2 domain from ethylene response element binding proteins 1 to 4 (Ohme-Takagi and Shinshi, 1995); Z37504-R, translated cadmium-inducible Arabidopsis gene (GenBank accession number Z37504) AP2 domain; Z27045-R, translated Arabidopsis EST (GenBank accession number Z27045) AP2 domain; D47184-R, translated rice EST (GenBank accession number D47184) AP2 domain.

(B) Linker region. R1 and R2 represent the two AP2 domains flanking the linker sequences. The invariant glycine mutated in *ant-2* is indicated by the asterisk. The sequence of the rice EST, D23002, is incomplete, and the presence or absence of the AP2 domain R1 is unknown. ANT-L, ANT linker region; D15799-L, translated rice EST D15799 linker; AP2-L, AP2 linker; D23002-L, translated rice EST D23002 linker.

(Figure 2). Ovules from strong *ant* mutants do not produce a functional embryo sac, although it remains to be clarified whether the megasporocytes present in these ovules undergo meiosis. Megasporocytes within ovules of the weak *ant-3* mutant do appear to undergo megasporogenesis to produce a single megaspore (Figure 2F). However, a viable female gametophyte is not usually formed. Instead, both *ant-1* and *ant-3* ovules contain an abnormal proliferation of cells in the nucellus in place of an embryo sac (Figures 2H and 2I). These cells may be partly responsible for the ridge of tissue seen in mature *ant-1* ovules (Figure 1K), because they appear to cause some bulging of the ovule adjacent to the funiculus (Figure 2H). The origin of these proliferating cells is not clear. They may be nucellar cells that would normally be crushed by the developing female gametophyte but, in its absence, proliferate to fill the area usually occupied by the embryo sac. Tissue-specific markers in the ovule will be needed to identify the origin of these cells.

Whether the defective embryo sac development is a direct effect of loss of *ANT* activity in the premeiotic megasporocyte, an indirect effect due to the abnormal integument development, or a combination of the two is not known. Integuments are thought to play both a structural and nutritional role in the development of the embryo sac and may be involved in communication between the diploid ovule and the haploid female gametophyte (Reiser and Fischer, 1993). The fact that *ant*, *bel1*, and *sin1* plants all show abnormal integument and female gametophyte development suggests that the two processes are interdependent (Robinson-Beers et al., 1992; Lang et al., 1994; Modrusan et al., 1994). Recently, Reiser et al. (1995) have shown that *BEL1* RNA is not detected in the female gametophyte, suggesting that the lack of an embryo sac in *bel1* plants

may be a secondary effect of defective integument development. Clearly, strong *ant* mutants, which lack both the inner and outer integuments, might not be expected to produce a functional embryo sac for any of the reasons discussed above. Less clear is the role of the integuments in *ant-3* female gametophyte development. Ovules from *ant-3* plants contain both the inner and outer integuments, often fully enclosing the nucellus (Figure 1M). If abnormal integument development is responsible for the nonfunctional embryo sacs in *ant-3* ovules, only subtle effects are needed.

In contrast to strong *ant* mutants, homozygous *ant-3* plants produce a very low level of viable seed (Table 1). This indicates that at least a few of the ovules in the *ant-3* mutant complete megagametogenesis to form a functional female gametophyte. This variable embryo sac development is environmentally sensitive, with increased fertility found when *ant-3* plants are grown under continuous light (H. Chow, unpublished results). The cause of this increased fertility remains to be determined. However, it is important to keep in mind that the *ant-3* mutation is caused by a T-DNA insertion within the promoter region of the *ANT* gene (Figure 6). Therefore, *ant-3* mutants should produce functional ANT protein, although at a reduced level. It is possible that, at a low frequency, some *ant-3* ovules have a transient increase in *ANT* expression, allowing for the development of a functional ovule and embryo sac.

Why do strong *ant* mutants fail to initiate inner and outer integument development? One model proposes the lack of an integument-specific domain within the developing ovule. This is unlikely to be the case, however, because in situ localization of the integument-specific marker *BEL1* indicated that an integument domain is produced in ovules from strong *ant* mutants (Figure 3D). These results suggest that *ANT* may function during the initiation of integument morphogenesis, after the apical–basal pattern (nucellus, integuments, funiculus) has formed in the developing ovule. Analysis of *ant-1 bel1-2* double mutants (Figure 3B) suggests that after *ANT* initiates outer integument development, *BEL1* is required to specify its identity. The relationship between *ANT* and *BEL1* in the development of the inner integument cannot be determined from analysis of *ant-1 bel1-2* double mutants, because both *ant-1* and *bel1-2* single mutants fail to initiate inner integument development.

ANT Has a Role in Floral Organ Development

In addition to the ovule defects, mutations in *ANT* can also affect other aspects of flower development (Figures 4 and 5). This is most clearly illustrated in the phenotype of flowers from strong *ant* mutants, consisting of a random loss and abnormal morphology of organs in the first three whorls. A similar flower phenotype was described for the *tousled* mutation of Arabidopsis (Roe et al., 1993). The organ loss in *ant* flowers may be due to a failure to initiate floral organ primordia, as was found for *tousled*, or the organs may be initiated but then abort soon after. Analysis of early floral meristem development is needed to address this issue. In contrast to the strong *ant* mutants, the weak *ant-3* mutant has flowers with only minor differences from the wild type (Figures 4B and 5). However, *ant-3* is almost completely sterile under standard growth conditions. This indicates that the sterile phenotype is separable from the flower phenotype and not due to downstream effects of abnormal flower development.

It is interesting that the putative null mutant, *ant-1*, has such a variable flower phenotype. Why a null mutation causes a random loss of organs in each whorl is unclear. It may be that there is some redundancy for *ANT* function in flower development. This is particularly intriguing given the homology between *ANT* and *AP2* (Figure 9). It is conceivable that *ANT* and *AP2*, or some other member of the AP2 domain family, have overlapping functions in flower development. Analysis of *ant ap2* double mutants may be informative in this regard. However, because of the tight linkage between *ANT* and *AP2*, *ant ap2* double mutants will be difficult to obtain (see Methods). Partially redundant activities have been described previously for *APETALA1* and *CAULIFLOWER*, both MADS box genes involved in floral meristem formation (Bowman et al., 1993; Kempin et al., 1995). However, given the severe ovule phenotype in *ant-1* plants, there is unlikely to be a redundant function for *ANT* in the ovule.

Combined, these results suggest that the *ANT* gene product is needed at certain critical levels to control flower, ovule, and female gametophyte development. In its absence, many aspects of flower development are altered, with ovule integument and female gametophyte development dramatically suppressed. Low levels of active *ANT* RNA result in relatively normal flowers, with nonfunctional ovules that specifically lack a female gametophyte.

The need for a certain threshold of *ANT* activity to produce functional ovules may explain why the complemented *ant-3* plants were not restored to full fertility (Table 1). The insertion of new genetic material into plant genomes can alter the expression of both newly introduced and endogenous genes (Matzke and Matzke, 1995). In addition, the position of the inserted transgene in the plant genome can affect the level of transgene expression (Dean et al., 1988; Peach and Velten, 1991). Potentially, either or both of these effects could be responsible for insufficient levels of the *ANT* gene product in the complemented plants to restore wild-type levels of fertility.

Alternatively, we may be lacking an essential regulatory element in the genomic fragment used for complementation (Figure 6), although this would suggest a lengthy promoter region because 4 kb upstream of the transcription start site was included. Partial complementation of an Arabidopsis mutant has been reported previously (Callos et al., 1994).

The *ANT* Gene Product Is a Member of a New Class of DNA Binding Proteins

The ANT protein was found to contain a recently described motif, the AP2 domain (Figure 9A; Jofuku et al., 1994). The AP2 domain is related to the DNA binding domain of ethylene response element binding proteins (EREBPs), a small family of DNA binding proteins from tobacco (Ecker, 1995; Ohme-

Takagi and Shinshi, 1995; Weigel, 1995). EREBPs were isolated due to their ability to bind to an ethylene response element found in a number of pathogenesis-related protein genes (Ohme and Shinshi, 1990; Eyal et al., 1993; Hart et al., 1993; Ohme-Takagi and Shinshi, 1995).

Sequence analysis indicated that the AP2 domain family of proteins can be subdivided into two groups: one group containing a single domain (i.e., EREBPs), and the second group containing two AP2 domains and a conserved linker region (i.e., ANT and AP2). For AP2, both of the AP2 domains were crucial for full activity because point mutations near the conserved core region of either domain resulted in an *ap2* phenotype (Jofuku et al., 1994). The region linking the two AP2 domains is also likely to be important for protein activity due to its conservation in proteins containing two AP2 domains (Figure 9B). A single point mutation in the strong *ant-2* allele, altering a conserved glycine in the linker region to aspartic acid, causes a phenotype similar to that conferred by the null allele, *ant-1*, also indicating the critical importance of this region for ANT activity.

Multiple DNA binding domains are usually required for site-specific recognition (Pabo and Sauer, 1992). The presence of an additional DNA binding domain in ANT (the second AP2 domain) may increase the affinity and/or alter the specificity of the protein–DNA interactions compared with proteins that contain only a single DNA binding domain (Sturm and Herr, 1988; Verrijzer et al., 1992; Del Rio et al., 1993). The second AP2 domain will also add an additional amphipathic α-helix. Amphipathic α-helices are structural elements that create a dimerization interface in a number of DNA binding proteins (Baxevanis and Vinson, 1993). The addition of a second amphipathic α-helix may result in more stable protein–protein interactions or alter the specificity of those interactions (Baxevanis and Vinson, 1993; Ferre-D'Amare et al., 1993).

The AP2 domain is found in a variety of plant species based primarily on translation of cDNA sequences present in gene data bases. A translated rice EST, D15799, was the most similar to ANT among all known members of this family of proteins, suggesting that this gene might be an *ANT* ortholog in rice. It was pointed out recently that a second rice EST, D23002, might be an *AP2* ortholog, based on sequence homology (Figure 9; Weigel, 1995). A putative maize *ANT* ortholog has also been found in the gene data base (GenBank accession number Z47554). This suggests that both *ANT* and *AP2* are likely conserved in plants as distantly related as dicotyledons and monocotyledons.

ANT maps to the same approximate location on chromosome 4 as *AP2*, the closest *ANT* relative in Arabidopsis. This suggests that a gene duplication occurred to form *ANT* and *AP2* and that other genes in the AP2 domain family may also map to this region of chromosome 4. It will be interesting to determine whether *ANT* and *AP2* orthologs in rice are also genetically linked in the rice genome.

Surprisingly, given the prevalence of genes encoding AP2 domain proteins in the plant data base, searches have failed to identify genes encoding this motif in organisms other than plants. This leads to interesting questions about the evolution of these genes. Could genes encoding AP2 domain proteins have coevolved with plant-specific pathways? EREBPs are almost surely involved in plant hormonal signal transduction, binding to DNA sequences required for the induction of pathogenesis-related protein genes in response to ethylene (Ohme-Takagi and Shinshi, 1995). In addition, *AP2* has been reported to be potentially involved in the gibberellin signal transduction pathway (Okamuro et al., 1993). Whether roles in plant hormone signal transduction will be a general phenomenon for AP2 domain proteins remains to be determined.

The presence within ANT of a putative DNA binding domain, serine-threonine–rich region, and potential nuclear localization site suggests that ANT is a likely transcriptional regulator. Potential downstream targets for ANT include genes involved in flower, integument, and female gametophyte development. Identification of ANT DNA binding sequences may allow detection of ANT targets.

ANT Gene Expression Is Not Restricted to Floral Tissue

RNA gel blot analysis indicated that *ANT* gene expression was found in both floral and vegetative tissue (Figure 7B). Expression in a wide range of organs appears to be a common occurrence for AP2 domain genes (Jofuku et al., 1994; Ohme-Takagi and Shinshi, 1995; J. Okamuro and D. Jofuku, personal communication). As expected, the highest level of *ANT* expression was seen in developing flowers (stages 0 to 12). This is both the time and place of ovule development. However, expression was also found in both the aerial portion and roots of nonflorally induced seedlings. *ANT* expression in these tissues is puzzling because no obvious phenotype was seen in the growth of *ant* mutants before floral induction. One possible explanation is that there are genes with redundant functions in these organs, as was discussed for *ANT*'s role in flower development. Alternatively, different growth conditions might illuminate a role for *ANT* in the vegetative phase of plant development not seen in our standard growth conditions. We cannot definitively rule out cross-hybridization to other AP2 domain gene family members, because the probe used in these experiments contained the AP2 domain coding region. However, we did not detect cross-hybridization to the closest known Arabidopsis family member, *AP2*, because the *AP2* transcript is 1.6 kb in length (Jofuku et al., 1994), which is smaller than the 2.25-kb *ANT* transcript (Figure 7). In addition, *ANT* RNA was not detected in rosette leaf tissue, where *AP2* is known to be expressed (Jofuku et al., 1994). Similar examples of expression in plant tissues with no obvious phenotype have been described. These include the *AP2* and *LEAFY* genes required for floral development in Arabidopsis (Weigel et al., 1992; Jofuku et al., 1994). The *BEL1* gene was also found to be expressed in vegetative organs in which no phenotype was described (Reiser et al., 1995).

In conclusion, ANT is a new member of a family of proteins that play a crucial role in a number of plant developmental processes. Molecular dissection of ANT will begin to reveal how this class of proteins functions.

METHODS

Plant Material and Genetic Analysis

aintegumenta mutants (*ant-1*, *ant-2*, and *ant-3*) were identified from a collection of independently isolated *Arabidopsis thaliana* (ecotype Wassilewskija) lines transformed with *Agrobacterium tumefaciens* (Feldmann, 1991). *ant-1* and *ant-3* were originally referred to as *ovm3* and *ovm2*, respectively (Reiser and Fischer, 1993). *ant-2* was a gift from G. Haughn (University of British Columbia, Vancouver, Canada). Progeny from self-pollinated heterozygous *ant* plants were analyzed for segregation of sterility. An *ant-1* segregating population contained 385 fertile and 121 sterile plants (3:1, $\chi^2 = 0.32$, $P > 0.5$), an *ant-2* segregating population contained 81 fertile and 32 sterile plants (3:1, $\chi^2 = 0.66$, $P > 0.3$), and an *ant-3* segregating population contained 390 fertile and 131 sterile plants (3:1, $\chi^2 = 0.01$, $P > 0.9$). These tests indicated that each *ant* mutant was due to a single recessive nuclear mutation. In addition, each sterile plant in the *ant-1* and *ant-2* segregating populations displayed the flower phenotype described in Results.

Allelism tests were conducted using a heterozygous female and a homozygous male. The F_1 progeny of *ANT-3/ant-3* × *ant-1/ant-1* were 14 fertile and 14 sterile (1:1), whereas the reciprocal cross, *ANT-1/ant-1* × *ant-3/ant-3*, produced three fertile and four sterile plants (1:1, $\chi^2 = 0.14$, $P > 0.7$). The F_1 progeny of *ANT-2/ant-2* × *ant-3/ant-3* were 15 fertile and 23 sterile (1:1, $\chi^2 = 1.6$, $P > 0.2$). These tests indicated that *ant-1*, *ant-2*, and *ant-3* are allelic.

The map position of the *ANT* gene was determined by a genetic cross of *ant-3/ant-3* to a chromosome 4 marker line (*bp/bp*, *cer2/cer2*, and *ap2/ap2*). We failed to identify any recombinants between *AP2* and *ANT* in our analysis of 400 F_2 progeny, suggesting tight linkage to *AP2* on the lower arm of chromosome 4.

Plants were routinely grown on Sunshine Mix (Fisons Horticulture Inc., Vancouver, Canada) under standard greenhouse conditions (16-hr light cycle, 20 to 22°C), except where otherwise indicated.

ant-1 bel1-2 Double Mutant Construction

For construction of *ant-1 bel1-2* double mutants, *ant-1/ant-1* plants were crossed to *BEL1-2/bel1-2* plants. The F_1 progeny were allowed to self, and the F_2 generation were scored for ovule phenotype. As expected, 50% of the F_1 progeny produced segregating populations of *bel1-2* and *ant-1* plants in the next generation and 50% produced only a segregating population of *ant-1* plants. A large-scale analysis of the F_2 progeny from those F_1 progeny that produced segregating populations of *bel1-2* and *ant-1* plants gave 608 wild-type plants, 264 *ant-1* plants, and 186 *bel1-2* plants. No novel phenotypes were detected. These results suggested that *ant-1 bel1-2* double mutants were being scored as *ant-1* mutants (9:4:3, $\chi^2 = 0.8$, $P > 0.5$). Four putative double mutant plants were identified using polymerase chain reaction (PCR); plants looked like *ant-1* and had a *bel1-2*–specific band, using *BEL1*-specific primers (Reiser et al., 1995). These were crossed to wild-type plants (F_1 will be heterozygous at both loci, and the F_2 will segregate for both phenotypes) to confirm the genotypes. Two lines analyzed segregated for both *ant-1* and *bel1-2* in the expected proportions, confirming the genotypes.

Microscopy

Plants for microscopy were grown on Sunshine Mix in growth chambers (Percival Manufacturing Co., Boone, IA) at 22°C with a 16-hr light cycle. Staging of flower development was determined, as described by Smyth et al. (1990). For wild-type and *ant* plants, dissected gynoecia at different stages of development were fixed in 3% glutaraldehyde in 0.02 M sodium phosphate buffer, pH 7.0, at room temperature for 24 hr. The fixed samples were rinsed in buffer and dehydrated in a graded ethanol series. For scanning electron microscopy, the dehydrated samples were critical point dried in liquid CO_2 and mounted on aluminum stubs. The samples were sputter-coated with 30 nm of gold and examined with a scanning electron microscope (ISI-DS130; International Science Instrument, Pleasanton, CA). Photographs were taken with high resolution film (type 55; Polaroid, Cambridge, MA).

For light microscopy, gynoecia were fixed and dehydrated as described above and embedded in JB-4 Plus embedding resin (Polysciences, Warrington, PA). Sections (2-μm thick) were cut with glass knives, stained with periodic acid and Schiff's reagent (Sigma), and poststained with aqueous toluidine blue solution (1%). Photographs were taken using bright-field optics and Kodak Royal Gold 100 color film on an Axiophot microscope (Zeiss, Göttingen, Germany).

Flowers from *ant-1 bel1-2* plants and *bel1-2* plants were fixed overnight in ethanol–acetic acid (9:1 [v/v]) and then cleared in 2.5 kg/L chloral hydrate. Cleared ovules were observed with a Zeiss Axioskop and photographed with a Nikon (Melville, NY) 6006 camera.

Scanning electron micrographs, clearings, and sections for in situ hybridization were scanned into a computer, using a Microtek scanner (Microtek International, Inc., Hsinchu, Taiwan). Pictures were processed for publication using Adobe Photoshop 3.0 (Adobe Systems Inc., Mountain View, CA) and printed on a Tektronix Phaser 400 color printer (Tektronix Inc., Wilsonville, OR).

In Situ Hybridization

Tissues for in situ hybridization were fixed and embedded as previously described by Drews et al. (1991). Sections (8-μm thick) were adhered to Probe On Plus slides (Fisher Scientific, Pittsburgh, PA) at 42°C overnight. In situ hybridization was performed using riboprobes labeled with digoxigenin according to the manufacturer's instructions (Boehringer Mannheim). For *BEL1*, the clone pLR115 (Reiser et al., 1995) was used to generate an antisense transcript. Hybridization and detection with nitro blue tetrazolium and X-phosphate were performed with a modified Genius protocol (Boehringer Mannheim; G. Drews, personal communication). Sections were photographed on a Zeiss Axioskop, using differential interference contrast and bright-field optics.

DNA Methods

Standard cloning procedures were performed, as described by Sambrook et al. (1989). Plant genomic DNA was isolated using a scaled-up version of the method described by Dellaporta et al. (1983), including a final CsCl centrifugation step. Alkali blotting of DNA to Hybond N+ membranes was performed as described by the manufacturer (Amersham). Probes used for hybridization were labeled using the Prime-It II kit and ^{32}P-dCTP, as recommended by the manufacturer (Stratagene). Prehybridization, hybridization (at 65°C), and washes were essentially as described by Church and Gilbert (1984).

Construction and Screening of Genomic and cDNA Libraries

Sau3A partially digested homozygous *ant-3* genomic DNA was cloned into XhoI-digested λGEM-11 and packaged as recommended by the manufacturer (Promega). A wild-type Arabidopsis (ecotype Wassilewskija) genomic library in λGEM-11 was a gift of K. Feldmann (University of Arizona, Tucson). An Arabidopsis (ecotype Landsberg

erecta) flower cDNA library was a gift of E. Meyerowitz (California Institute of Technology, Pasadena). Screening and plaque purification of *ant-3* genomic, wild-type genomic, and flower cDNA libraries were performed as described by Ausubel et al. (1992). In vivo excision of plaque-purified cDNA clones was performed as described by the manufacturer (Stratagene).

5′ Rapid Amplification of cDNA Ends

5′ Rapid amplification of cDNA ends (RACE) (Frohman et al., 1988) was performed using a 5′ RACE kit, as described by the manufacturer (Gibco BRL). Briefly, 500 ng of polyadenylated RNA from developing flowers (stages 0 to 12) of wild-type Arabidopsis was used as a template for first-strand cDNA synthesis, using gene-specific primer 1 (5′-GTGACTTGTGTTGTTGTGATGGG-3′). The resulting cDNA strand was tailed using terminal transferase and dCTP, and PCR was performed using gene-specific primer 2 (5′-CAGAAGAAGAAGAAGTTGCAGCTG-3′) and the anchor primer (Gibco BRL). Taq DNA polymerase (Perkin-Elmer) was used for this and subsequent PCR. A second round of PCR, using gene-specific primer 3 (5′-TGAAGATGAGTAAATAGCTTC TCT-3′) and the universal anchor primer (Gibco BRL), was performed to amplify further the resulting DNA fragment. For first-strand cDNA synthesis and both rounds of PCR, the *ANT*-specific primers used were to regions 5′ of the AP2 domains. The resulting DNA was subcloned into pCRII by TA cloning (Invitrogen, San Diego, CA). Dideoxy sequencing was performed on multiple clones, using Sequenase 2.0 enzyme (U.S. Biochemical, Cleveland, OH) (Sanger et al., 1977).

Sequencing of *ant* Mutant Alleles

The *ANT* genomic region from *ant-1* and *ant-2* was isolated in segments by PCR, using gene-specific primers (Saiki et al., 1988). Initially, purified DNA from each allele was used as a template for PCR. Each amplified fragment was either sequenced directly, using a single-stranded sequencing kit (Pharmacia, Piscataway, NJ) or subcloned into pCRII by TA cloning. Regions that were found to contain mutations were subjected to a second round of PCR, using alkali-treated plant tissue as a template (Klimyuk et al., 1993). Amplified fragments were subcloned into pCRII for propagation and sequencing. Dideoxy sequencing was performed using the Sequenase 2.0 enzyme. When subcloned templates were used for sequencing, at least two individual clones were pooled and sequenced.

The *ANT* genomic region from the *ant-3* allele was isolated from the *ant-3* genomic library described above. The 3.7- and 2.0-kb HindIII fragments containing the *ANT* transcription unit (Figures 6 and 8B) were subcloned into pUC18 and sequenced, using an Applied Biosystems, Inc. (Foster City, CA) automated sequencer at the University of California, Berkeley, Sequencing Center.

Transformation of *ant* Plants

The *ANT* genomic construct used for complementation of homozygous *ant-3* plants was constructed by cloning a 10-kb SalI fragment from a wild-type λ clone (spanning the site of T-DNA insertion in *ant-3*) into pHygA to yield pKK18. pHygA, a precursor to plasmid MH856, contains a hygromycin resistance gene and an XhoI site in the polylinker (Honma et al., 1993). pKK18 was electroporated into Agrobacterium strain ASE (Rogers et al., 1987) for plant transformation, giving strain ASE-KK18.

Homozygous *ant*-3 mutant seed were obtained from selfed homozygous plants (*ant-3*/*ant-3*) grown under continuous light in which a low level of fertility was induced (H. Chow, unpublished results). Roots from ~50 homozygous *ant-3* seedlings were transformed with ASE-KK18, using the procedure described by Marton and Browse (1991). Selection was on Murashige and Skoog plates containing 15 mg/L hygromycin B (Calbiochem, LaJolla, CA). Hygromycin-resistant calli were rooted with 2 mg/L indolebutyric acid, transferred to soil, and allowed to set seed. DNA gel blot analysis was used to confirm the genotype of resulting transformants (data not shown).

RNA Methods

Total RNA was isolated from plant tissue, as previously described by Comai et al. (1992), and quantitated by spectrophotometry. Flower bud tissue from stage 0 to 12 (Smyth et al., 1990), open flowers (stage 13), young siliques, and mature rosette leaf tissue were harvested from 1-month-old plants grown in the greenhouse. Aerial and root tissue were harvested from seedlings grown under continuous light in a growth chamber for 9 and 10 days, respectively. Purification of polyadenylated RNA for the 5′ RACE procedure was performed by using the Oligotex system, as described by the manufacturer (Quiagen Inc., Chatsworth, CA). Electrophoresis of 20 μg of total RNA through a 1.2% (w/v) agarose/6.6% (w/v) formaldehyde gel was performed as described by Sambrook et al. (1989). Estimated RNA sizes were determined by comparison with known RNA standards (Gibco BRL). Transfer of RNA to Hybond N membranes and subsequent treatment were performed as recommended by the manufacturer (Amersham). Probes used for hybridizations were labeled using the Prime-It II kit and ^{32}P-dCTP, as recommended by the manufacturer. The *ANT* cDNA clone used for the RNA gel blots shown in Figure 7 contained *ANT* cDNA sequences from nucleotides 375 to 2148 (Figure 8A). Prehybridization, hybridization (at 65°C), and washes were essentially as described by Church and Gilbert (1984). Hybridization of the *ANT* cDNA probe (nucleotides 375 to 2148) to DNA gel blots at the same stringency used for RNA gel blots detected only minor cross-hybridization to other genes within the Arabidopsis genome (<3% of *ANT*-specific DNA bands; data not shown). A clone containing pea 18S rDNA sequences was used for control hybridizations (Jorgenson et al., 1987).

ACKNOWLEDGMENTS

We thank George Haughn for providing us with the *ant-2* allele, Chad Williams for genetic analysis of plants, Barbara Rotz for providing excellent greenhouse services, and Ann Fischer for initial sequencing of the *ant-3* allele. We also wish to thank John Harada, Jack Okamura, Diane Jofuku, Yang Pan, and Fischer laboratory members for their critical reading of the manuscript. This work was supported by National Science Foundation Grant No. IBN-9505813 to R.L.F. K.M.K. was supported by a National Institutes of Health National Research Service Award (No. F32-GM14869).

Received September 19, 1995; accepted October 30, 1995.

REFERENCES

Ausubel, F.M., Brent, R., Kingston, R.E., Moore, D.D., Seidman, J.G., Smith, J.A., and Struhl, K., eds (1992). Current Protocols

in Molecular Biology. (New York: Greene Publishing and Wiley-Interscience).

Baxevanis, A.D., and Vinson, C.R. (1993). Interactions of coiled coils in transcription factors: Where is the specificity? Curr. Opin. Genet. Dev. **3,** 278–285.

Bouman, F. (1984). The ovule. In Embryology of Angiosperms, B.M. Johri, ed (New York: Springer-Verlag), pp. 123–158.

Bowman, J.L., Smyth, D.R., and Meyerowitz, E.M. (1989). Genes directing flower development in *Arabidopsis.* Plant Cell **1,** 37–52.

Bowman, J.L., Smyth, D.R., and Meyerowitz, E.M. (1991). Genetic interactions among floral homeotic genes of Arabidopsis. Development **112,** 1–20.

Bowman, J.L., Sakai, H., Jack, T., Weigel, D., Mayer, U., and Meyerowitz, E.M. (1992). Superman, a regulator of floral homeotic genes in *Arabidopsis.* Development **114,** 599–615.

Bowman, J.L., Alvarez, J., Weigel, D., Meyerowitz, E.M., and Smyth, D.R. (1993). Control of flower development in *Arabidopsis thaliana* by *APETALA1* and interacting genes. Development **119,** 721–743.

Callos, J.D., DiRado, M., Xu, B., Behringer, F.J., Link, B.M., and Medford, J.I. (1994). The *forever young* gene encodes an oxidoreductase required for proper development of the *Arabidopsis* vegetative shoot apex. Plant J. **6,** 835–847.

Chelsky, D., Ralph, R., and Jonak, G. (1989). Sequence requirements for synthetic peptide-mediated translocation to the nucleus. Mol. Cell. Biol. **9,** 2487–2492.

Church, G., and Gilbert, W. (1984). *Genomic sequencing.* Proc. Natl. Acad. Sci. USA **81,** 1991–1995.

Comai, L., Matsudaira, K.L., Heupel, R.C., Dietrich, R.A., and Harada, J.J. (1992). Expression of a *Brassica napus* malate synthase gene in transgenic tomato plants during the transition from late embryogeny to germination. Plant Physiol. **98,** 53–61.

Dean, C., Jones, J., Favreau, M., Dunsmuir, P., and Bedbrook, J. (1988). *Influence of flanking sequences on variability of expression* levels of an introduced gene in transgenic tobacco plants. Nucleic Acids Res. **16,** 9267–9283.

Dellaporta, S.L., Wood, J., and Hicks, J.B. (1983). A plant DNA minipreparation: Version II. Plant Mol. Biol. Rep. **4,** 19–21.

Del Rio, S., Menezes, S.R., and Setzer, D.R. (1993). The function of individual zinc fingers in sequence-specific DNA recognition by transcription factor IIIA. J. Mol. Biol. **233,** 567–579.

Drews, G.N., Bowman, J.L., and Meyerowitz, E.M. (1991). Negative regulation of the *Arabidopsis* homeotic gene *AGAMOUS* by the *APETALA2* product. Cell **65,** 991–1002.

Ecker, J.R. (1995). The ethylene signal transduction pathway in plants. Science **268,** 667–675.

Eyal, Y., Meller, Y., Lev-Yadun, S., and Fluhr, R. (1993). A basic-type PR-1 promoter directs ethylene responsiveness, vascular and abscission zone-specific expression. Plant J. **4,** 225–234.

Feldmann, K.A. (1991). T-DNA insertion mutagenesis in Arabidopsis: Mutational spectrum. Plant J. **1,** 71–82.

Ferre-D'Amare, A.R., Prendergast, G.C., Ziff, E.B., and Burley, S.K. (1993). Recognition by Max of its cognate DNA through a dimeric b/HLH.Z domain. Nature **363,** 38–45.

Frohman, M.A., Dush, M.K., and Martin, G.R. (1988). Rapid production of full-length cDNAs from rare transcripts: Amplification using a single gene-specific oligonucleotide primer. Proc. Natl. Acad. Sci. USA **85,** 8998–9002.

Gaiser, J.C., Robinson-Beers, K., and Gasser, C.S. (1995). The Arabidopsis *SUPERMAN* gene mediates asymmetric growth of the outer integument of ovules. Plant Cell **7,** 333–345.

Gashler, A.L., Swaminathan, S., and Sukhatme, V.P. (1993). A novel repression module, an extensive activation domain, and a bipartite nuclear localization signal defined in the immediate-early transcription factor Egr-1. Mol. Cell. Biol. **13,** 4556–4571.

Hart, C.M., Nagy, F., and Meins, F.J. (1993). A 61 bp enhancer element of the tobacco β-1,3-glucanase B gene interacts with one or more regulated nuclear proteins. Plant Mol. Biol. **21,** 121–131.

Hill, J.P., and Lord, E.M. (1989). Floral development in *Arabidopsis thaliana*—A comparison of the wild type and the homeotic *pistillata* mutant. Can. J. Bot. **67,** 2922–2936.

Honma, M.A., Baker, B.J., and Waddell, C.S. (1993). High frequency germinal transposition of Ds^{ALS} in Arabidopsis. Proc. Natl. Acad. Sci. USA **90,** 6242–6246.

Hulskamp, M., Schneitz, K., and Pruitt, R.E. (1995). Genetic evidence for a long-range activity that directs pollen tube guidance in Arabidopsis. Plant Cell **7,** 57–64.

Irish, V.F., and Sussex, I.M. (1990). Function of the *apetala-1* gene during *Arabidopsis* floral development. Plant Cell **2,** 741–753.

Jofuku, K.D., den Boer, B.G.W., Van Montagu, M., and Okamuro, J.K. (1994). Control of Arabidopsis flower and seed development by the homeotic gene *APETALA2.* Plant Cell **6,** 1211–1225.

Jorgenson, R.A., Cuellar, R.E., Thompson, W.F., and Kavanagh, T.A. (1987). Structure and variation in ribosomal RNA genes of pea: Characterization of a cloned rDNA repeat and chromosomal rDNA variants. Plant Mol. Biol. **8,** 3–12.

Kempin, S.A., Savidge, B., and Yanofsky, M.F. (1995). Molecular basis of the *cauliflower* phenotype in *Arabidopsis.* Science **267,** 522–525.

Klimyuk, V.I., Carroll, B.J., Thomas, C.M., and Jones, J.D.G. (1993). Alkali treatment for rapid preparation of plant material for reliable PCR analysis. Plant J. **3,** 493–494.

Komaki, M.K., Okada, K., Nishino, E., and Shimura, Y. (1988). Isolation and characterization of novel mutants of *Arabidopsis thaliana* defective in flower development. Development **104,** 195–203.

Kunst, L., Klenz, J.E., Martinez-Zapater, J., and Haughn, G.W. (1989). *AP2* gene determines the identity of perianth organs in flowers of *Arabidopsis thaliana.* Plant Cell **1,** 1195–1208.

Lang, J.D., Ray, S., and Ray, A. (1994). *sin1*, a mutation affecting female fertility in Arabidopsis, interacts with *mod1*, its recessive modifier. Genetics **137,** 1101–1110.

Léon-Kloosterziel, K.M., Keijzer, C.J., and Koornneef, M. (1994). A seed shape mutant of Arabidopsis that is affected in integument development. Plant Cell **6,** 385–392.

Mansfield, S.G., Briarty, L.G., and Erni, S. (1990). Early embryogenesis in *Arabidopsis thaliana*: The mature embryo sac. Can. J. Bot. **69,** 447–460.

Marton, L., and Browse, J. (1991). Facile transformation of *Arabidopsis. Plant Cell Rep.* **10,** *235–239.*

Matzke, M.A., and Matzke, A.J.M. (1995). How and why do plants inactivate homologous (trans)genes? Plant Physiol. **107,** 679–685.

Modrusan, Z., Reiser, L., Feldmann, K.A., Fischer, R.L., and Haughn, G.W. (1994). Homeotic conversion of ovules into carpel-like structures in Arabidopsis. Plant Cell **6,** 333–349.

Ohme, M., and Shinshi, H. (1990). Structure and expression of a tobacco β-1,3-glucanase gene. Plant Mol. Biol. **15,** 941–946.

Ohme-Takagi, M., and Shinshi, H. (1995). Ethylene-inducible DNA binding proteins that interact with an ethylene-responsive element. Plant Cell **7,** 173–182.

Okamuro, J.K., den Boer, B.G.W., and Jofuku, K.D. (1993). Regulation of Arabidopsis flower development. Plant Cell **5,** 1183–1193.

Pabo, C.O., and Sauer, R.T. (1992). Transcription factors: Structural families and principles of DNA recognition. Annu. Rev. Biochem. **61,** 1053–1095.

Peach, C., and Velten, J. (1991). Transgene expression variability (position effect) of CAT and GUS reporter genes driven by linked divergent T-DNA promoters. Plant Mol. Biol. **17,** 49–60.

Ray, A., Robinson-Beers, K., Ray, S., Baker, S.C., Lang, J.D., Preuss, D., Milligan, S.B., and Gasser, C.S. (1994). *Arabidopsis* floral homeotic gene BELL (*BEL1*) controls ovule development through negative regulation of AGAMOUS gene (*AG*). Proc. Natl. Acad. Sci. USA **91,** 5761–5765.

Reiser, L., and Fischer, R.L. (1993). The ovule and the embryo sac. Plant Cell **5,** 1291–1301.

Reiser, L., Modrusan, Z., Margossian, L., Samach, A., Ohad, N., Haughn, G.W., and Fischer, R.L. (1995). The *BELL1* gene encodes a homeodomain protein involved in pattern formation in the Arabidopsis ovule primordium. Cell **83,** 735–742.

Robinson-Beers, K., Pruitt, R.E., and Gasser, C.S. (1992). Ovule development in wild-type Arabidopsis and two female-sterile mutants. Plant Cell **4,** 1237–1249.

Roe, J.L., Rivin, C.J., Sessions, R.A., Feldmann, K.A., and Zambryski, P.C. (1993). The *Tousled* gene in A. thaliana encodes a protein kinase homolog that is required for leaf and flower development. Cell **75,** 939–950.

Rogers, S.G., Klee, H.J., Horsch, R.B., and Fraley, R.T. (1987). Improved vectors for plant transformation: Expression cassette vectors and new selectable markers. Methods Enzymol. **153,** 253–277.

Saiki, R.K., Gelfand, D.H., Stoffel, S., Scharf, S.J., Higuchi, R., Horn, G.T., Mullins, K.B., and Ehrlich, H.A. (1988). Primer-directed enzymatic amplification of DNA with a thermostable DNA polymerase. Science **239,** 487–491.

Sambrook, J., Fritsch, E.J., and Maniatis, T. (1989). Molecular Cloning: A Laboratory Manual. (Cold Spring Harbor, NY: Cold Spring Harbor Laboratory Press).

Sanger, F., Nicklen, S., and Coulson, A.R. (1977). DNA sequencing with chain-terminating inhibitors. Proc. Natl. Acad. Sci. USA **74,** 5463–5467.

Schneitz, K., Hulskamp, M., and Pruitt, R.E. (1995). Wild-type ovule development in *Arabidopsis thaliana*: A light microscope study of cleared whole-mount tissue. Plant J. **7,** 731–749.

Seipel, K., Georgiev, O., and Schaffner, W. (1992). Different activation domains stimulate transcription from remote ('enhancer') and proximal ('promoter') positions. EMBO J. **11,** 4961–4968.

Shannon, S., and Meeks-Wagner, D.R. (1993). Genetic interactions that regulate inflorescence development in Arabidopsis. Plant Cell **5,** 639–655.

Smyth, D.R., Bowman, J.L., and Meyerowitz, E.M. (1990). Early flower development in *Arabidopsis*. Plant Cell **2,** 755–767.

Sturm, R.A., and Herr, W. (1988). The POU domain is a bipartite DNA-binding structure. Nature **336,** 601–604.

Verrijzer, C.P., Alkema, M.J., van Weperen, W.W., Van Leeuwen, H.C., Strating, M.J.J., and van der Vliet, P.C. (1992). The DNA binding specificity of the bipartite POU domain and its subdomains. EMBO J. **11,** 4993–5003.

Weigel, D. (1995). The APETALA2 domain is related to a novel type of DNA binding domain. Plant Cell **7,** 388–389.

Weigel, D., Alvarez, J., Smyth, D.R., Yanofsky, M.F., and Meyerowitz, E.M. (1992). *LEAFY* controls floral meristem identity in Arabidopsis. Cell **69,** 843–859.

Willemse, M.T.M., and Van Went, J.L. (1984). The female gametophyte. In Embryology of Angiosperms, B.M. Johri, ed (New York: Springer-Verlag), pp. 159–196.